Conference Proceedings

Solar World Congress 2015

Daegu, Korea, 08 – 12 November 2015

3D Shape Measurement of Solar Concentrator Based on Orthogonal Fringe Reflection Method

Huibin Zhu[1], Zhifeng Wang[1], Jianhan Zhang[1] and Qiang Yu[1]

[1] Key Laboratory of Solar Thermal Energy and Photovoltaic System, Institute of Electrical Engineering, Chinese Academy of Sciences, Beijing 100190, China

Abstract

Fringe reflection technique is an effective tool to measure the solar concentrator surface slopes, and then reconstruct the surface shape from gradient. However, most of the fringe reflection systems are based on four-step phase shifting method, which need eight figures at least. In order to increase the measurement speed, a new orthogonal fringe reflection method is proposed to measure the shape of solar concentrator, which requires only two fringe images to complete the 3D shape measurement of solar concentrator. The performance of this 3D shape measurement system is demonstrated with experiments.

Keywords: *Shape measurement; Orthogonal fringe reflection; Solar concentrator*

1.Introduction

In a concentrating solar plant, the solar field consisting of a large number of collectors, which collects and concentrates the solar energy onto the receiver, is the major cost component of a plant. To obtain a homogeneous flux distribution on the receiver, the collectors shape must be highly precise to low the energy losses. The ideal shape and optical efficiency of the collector maximizes the energy input of the receiver and has a high impact on the plant performance. Therefore, it is very important to test and evaluate the quality of the surfaces for guaranteeing the optical performance. However, due to technical restraints in the manufacturing and installing process, deviations from the optimum collector shape leading to energy losses on the receiver cannot be completely avoided. On the other hand, it is necessary to measure and adjust the optical quality of the collectors in the manufacturing process. To test and qualify the collectors, a measurement tool for measuring the surface profile with adequate precision should be needed.

Many different techniques for shape measurement of solar collectors have been proposed by a variety of researchers in the past decades. In 1978, Sandia National Laboratories presented a measurement system based on a laser ray trace tester for solar parabolic trough collectors[1]. This system scanned the surface with a laser beam, detected the reflected beam on a target and obtains the normal of the collector surface. This system is sufficiently accurate, but the setup is time consuming and the implementation to large surfaces might be difficult. This limitation is overcame by photogrammetry which measure 3D shapes by calculating the coordinates of the collector surface based on a series of photographies of collector taken from different positions[2]. This method is also time consuming and not suitable for large surfaces since the measured surface has to be equipped with a large number of target points. Recently, Ulmer et al. developed a new

doi:10.18086/swc.2015.04.06 Available at http://proceedings.ises.org

method for measuring the slope error of heliostat based on deflectometry[3-6,22]. Later, we use the similar approach combined with temporal phase unwrapped technique and novel easy calibration method to measure the heliostat facet[7,21]. And there are some other methods to measure the shape of solar collector, which are shown in [8-16]. Most of the fringe reflection systems are based on four-step phase shifting method, which need eight figures at least. In order to increase the measurement speed, a new orthogonal fringe reflection method is proposed to measure the shape of solar concentrator, which requires only two fringe images to complete the 3D shape measurement of solar collector, and is very fast compared with the four-step phase shifting method.

On the other hand, one of the major challenges in fringe-reflection measurement is to realize the shape reconstruction efficiently. In several cases it is sufficient to know the local gradient; however, it is also important to obtain the height information of the solar collector as well. If the shape is known, it is easy to align the collector according to the measured shape results. To obtain the shape of the solar collector, a numerical shape reconstruction method is needed. Essentially there are two different approaches for integration: local and global integration techniques [17,18]. Local method: it integrates along predetermined paths. The advantage of this method is that it is simple and fast. However, the locality of calculation causes a high dependency from data accuracy, and the propagation of height increments along paths also means propagation of errors. Global method: it tries to minimize a designed cost function. The advantage of this method is that there is no propagation of error. But the implementation has certain difficulties and somehow is not easily convergent. So, the desired surface reconstruction method should have the properties of both local and global integration methods; it needs to preserve local details without propagating the error along a certain path. In order to handle this problem, we choose a generalized Hermite interpolation approach employing radial basis functions (RBFs) for the shape reconstruction from the gradient data. This method has the advantage that it can be applied to scattered data. It allows us to integrate data sets with holes, irregular sampling grids, or irregularly shaped boundaries [19]. Finally, the performance of this 3D shape measurement system is demonstrated with experiments.

2.Principle of fringe reflection method

The optical properties of solar collector such as reflectivity do not allow us to apply the direct structured light illumination principle, because the projected structured light is reflected along the mirror direction and no light reaches the CCD sensors. However, it is possible to capture the reflective structured light and obtain the surface information of solar collector based on the fringe reflection technique. The main idea of this reflection technique is that: a fringe pattern generated by the computer can be projected onto a target screen, and the distorted fringe pattern from the solar collector is captured by the CCD camera, which is reflected by the surface under test. The distortion of the fringe pattern depends on the local slope variations and the height of the surface. By establishing the mathematical models, which combine the phase difference between the corresponding point on the reference surface and the measured object, the surface height and slope, the shape of the measured solar collector surface can be determined based on approximation employing radial basis functions discussed below. The schematic diagram of this measurement principle is shown in Figure 1.

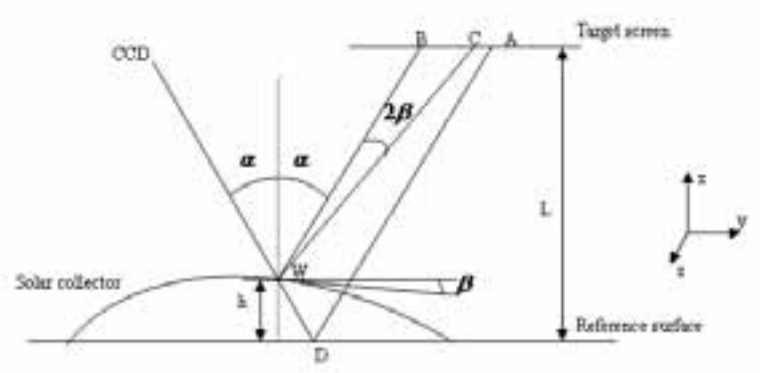

Figure 1: The schematic diagram of fringe reflection technique.

Figure 1 shows the optical configuration of the measured system. A fringe pattern generated by computer from a DLP projector is reflected off the solar collector and captured by CCD camera. The camera sees point A on the target screen with fringe pattern through the reference surface point D. Because of the solar collector surface with height value h and tilted at an angle β in the y direction, the collector surface point W reflects point C on the target screen. It is easy to obtain that the distance difference between the reflected point A and surface point C is related to the surface height and slope in both x and y direction. In this paper, the phase-shift profilmetry can be used to determine this difference. Based on the geometrical configurations in Figure 1, the relationship between the phase difference $\Delta\varphi(x,y)$, the slope $\tan\theta$ and the height h of the collector surface can be established as [24]:

$$\theta_x(x,y)=\frac{\Delta\varphi_x(x,y)p_x}{2\pi(L-h)}$$
$$\theta_y(x,y)=\frac{\Delta\varphi_y(x,y)p_y}{2\pi\sec(\alpha)^2(L-h)+\Delta\varphi_y(x,y)p_y\tan(\alpha)} \quad (1)$$

where (x,y) is the pixel coordinate, $\theta_x(x,y)$ and $\theta_y(x,y)$ are the angles of the measured surface in the x and y directions, respectively, L is the height of the target screen to the reference surface, α is the angle of the camera, $\Delta\varphi_x(x,y)$ and $\Delta\varphi_y(x,y)$ are the phase difference, p_x and p_y are the period of the fringes projected onto the screen in the x and y directions, respectively, h is the height from surface point W to the reference surface. The pattern phase distribution of each observed point can be evaluated by the phase retrieved method.

3.Orthogonal fringe reflection method

Although the phase-shifting method which need eight figures at least is an effective tool to measure the solar concentrator surface slopes, reasonable faster way to obtain both horizontal and vertical phase maps from a single fringe image. In this section, a new orthogonal fringe reflection method is proposed to measure the shape of solar concentrator, which is designed as a two-directional fringe pattern shown in Fig. (2) and requires only two fringe images to complete the 3D shape measurement of solar concentrator. The orthogonal fringe pattern can be expressed as

$$I(x,y) = 255\left[0.5 + 0.25\cos\left(2\pi\frac{x}{p_x}\right) + 0.25\sin\left(2\pi\frac{y}{p_y}\right)\right] \tag{2}$$

where p_x and p_y are fringe periods in the horizontal and vertical directions. The fringe phase values in both x and y directions can be calculated by the two-dimensional windowed fourier ridges method.

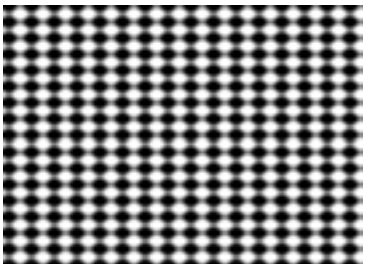

Figure 2: Orthogonal fringe

4.System calibration

The system calibration is very important in the shape measurement, because several different devices and objects are involved in the measurement system, such as CCD camera, projector, target screen, solar collector. Firstly, the CCD camera can be calibrated precisely by Tsai algorithm to provide the intrinsic and extrinsic parameters by using the checkerboard pattern. The system information about pixel size in both x and y directions, rotation angles and translational components for the transform between the measurement screen and the camera coordinate can be obtained. The next calibration algorithm is the reference plane calibration. This requires the measurement of the flat reference surface with respect to the camera position and involves the measurement of the phase distribution of the flat reflective surface across the measurement scene. This reference phase distribution is required in order to obtain the correct phase shift information from the measurement object. A novel virtual reference plane based on Zernike polynomials fitting method is presented. In the measurement system, the phase difference between the reference surface and collector surface should be determined. Because the solar collector is large, it is not easy to directly obtain the reference surface phase as size as the measured object. In order to solve this problem, the Zernike polynomials fitting method can be used to obtain the reference phase distribution: a small flat surface acts as reference plane, based on the phase distribution of the flat surface in both horizontal and vertical directions and Zernike polynomials fitting method, the phase distribution of virtual reference plane in the field of view during the whole measurement operation can be fitted. Once the calibration is finished, the system is ready for measurement.

5.Shape reconstruction

From Equation (1), it is easy to find out that not only the slopes but also the height of the collector surface has an influence on the position of the observed point on the screen. In order to obtain the height of object, we should reconstruct the collector shape from gradient data, which is very important to absolutely measure and evaluate the optical character of solar collector. To reconstruct the shape, one has to use the numerical integration method. But, most existing methods have different drawbacks: they either suffer from error propagation, or they introduce global errors due to unknown boundary conditions. The desired shape reconstruction method should have both local and global integration methods, which means that it should preserve the local details without propagating the error along a certain path. In this paper, the interpolation approach is used to reconstruct the shape from gradient data[19]. The gradient data is given as

pairs $(p_x(X_i), p_y(X_i))$, where $p_x(X_i)$ and $p_y(X_i)$ are the measured slopes of the collector at X_i in x and y directions, respectively ($1 \le i \le N$). Define the interpolate to be

$$z(X) = \sum_{i=1}^{N} \alpha_i \phi_x(X - X_i) + \sum_{i=1}^{N} \beta_i \phi_y(X - X_i) \tag{3}$$

where α_i and β_i are coefficients and ϕ is a radial basis function. ϕ_x and ϕ_y denote the analytic derivative of ϕ with respect to x and y , respectively. To obtain the coefficients in Equation (3), the analytic derivatives of the interpolate ϕ with the measured gradient data are matched as:

$$z_x(X_i) = p_x(X_i);\ z_y(X_i) = p_y(X_i); \tag{4}$$

The coefficients can be determined by solving the following linear equations:

$$\begin{pmatrix} \phi_{xx}(X_j - X_i) & \phi_{xy}(X_j - X_i) \\ \phi_{xy}(X_j - X_i) & \phi_{yy}(X_j - X_i) \end{pmatrix} \begin{pmatrix} \alpha_i \\ \beta_i \end{pmatrix} = \begin{pmatrix} p_x(X_i) \\ p_y(X_i) \end{pmatrix} \tag{5}$$

Based on the resulting coefficients α_i and β_i , the collector surface can be reconstructed by using the interpolate in Equation (3). The radial basis function ϕ can be chosen to be the Wendland's function[20] :

$$\phi(r) = \frac{1}{3}(1-r)_+^6(35r^2 + 18r + 3), r = \sqrt{x^2 + y^2} \tag{6}$$

This has two reasons for choosing the function. Firstly, Wendland's function allows one to choose their continuity according to the smoothness of the given data. This function is in $C^4(R_+)$ and leads to an interpolant, which is three times continuously differentiable and guarantees the integrability condition. Secondly, the compact support of the function allows one to adjust the support size in such a way that the solution of Eq. (5) is stable in the presence of noise [19]. To achieve this, one has to choose an appropriate scaling factor ρ. In [23], the authors showed that with an increasing support radius the interpolation error (i.e., the deviation from the measured slope data) increase, while the evaluation error (the deviation of the reconstructed shape) decreases. A larger support radius leads to more stable reconstruction in the presence of noise.

In the measurement, the amount of data is rather large. To solve such large data, the following method is presented: firstly, the data sets are split into a set of overlapping patches. On each patch, the data is interpolated and the calculated up to a constant of integration. Secondly, the least-squares fitting scheme is used to obtain the reconstructed surface on the entire field.

In Equation (1), both parameters L and α are unknown, an iterative strategy is applied to obtain the shape of measured collector surface:

1) Calculate the phase difference $\Delta\varphi_x$;
2) Let the height $z^0 = 0$, calculate the gradient $\tan\theta$ from Equation (1);
3) Reconstruct the height z^m of each patches from the gradient data, then obtain the entire field shape based on fitting scheme;
4) Calculate the difference between the adjacent iterative results $\Delta = z^m - z^{m-1}$;

5) If Δ is bigger than the iterative termination condition, calculate the gradient data from Equation (1) again. Then, return step 3); Otherwise, go to step 6);
6) Iterative terminate, recover the shape of collector.

In order to demonstrate the ability of proposed method, a simulation is conducted. The simulated function is defined by

$$z = 3(1-x)^2 \, \mathrm{e}^{(-x^2-(1+y)^2)} - 10(\frac{x}{5} - x^3 - y^5) \, \mathrm{e}^{(-x^2-y^2)} - \frac{1}{3}\mathrm{e}^{(-(1+x)^2-y^2)} \tag{7}$$

where the in-plane dimension x and y are both limited within a range from -3 to 3 mm with a sampling of 200×200 points. The true height is shown in Figure 3. The radial basis function integration method is used to integrate the shape within 13×13 subsets with a subset size of 20×20 and 25% overlap between neighboring subsets. Figure 4 (a) depicts the reconstructed shape on overlapping patches. Figure 4(b) and (c) show the reconstructed shape and the reconstructed height error. The deviation of height errors (RMS) is only less than 6×10^{-4} mm.

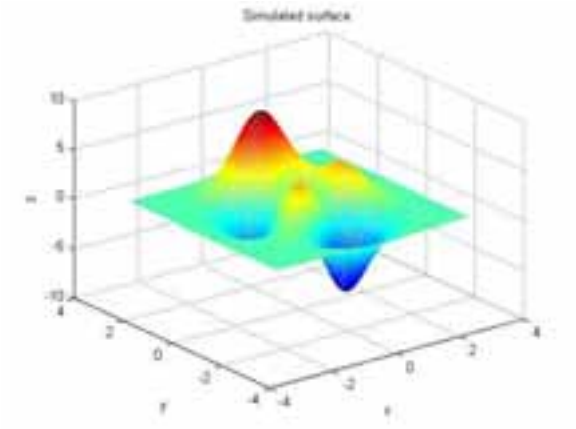

Figure 3: Simulated surface.

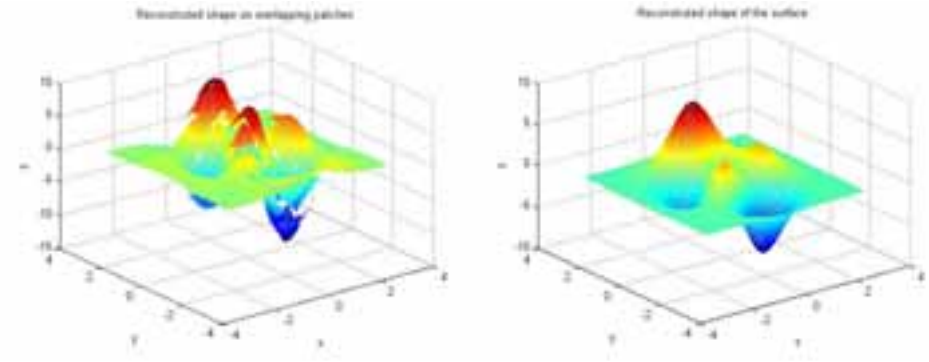

(a) (b)

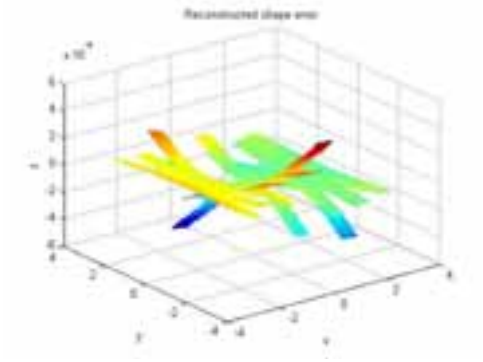

(c)

Figure 4: (a) Reconstructed shape on the overlapping patches; (b) Reconstructed shape of surface; (c) Reconstructed shape error.

6.Experiment

An experimental investigation of the feasibility of the proposed method is carried out as well. A RP3 inner mirror is measured with the fringe reflection technique. Figure 5(a) shows the two-dimensional pattern on the screen, which is projected on the target screen, the distorted patterns are captured by CCD camera (shown in Fig.5(b)). Figure 6 (a) - (d) show the slope distribution and slope error in both x and y directions, respectively, in which the local discontinuous areas are due to the phase unwrapped algorithm of the two-dimensional pattern. The slope errors (RMS, deviation from the ideal slope of shape) are: 2.6129mrad (x-direction), 0.1460mrad (y-direction). The proposed reconstructed method is then utilized to integrate the gradient data to reconstruct the shape of collector, which is shown in Figure 7 (a). In Fig. 7(b), it is the reconstruction error, (deviation from the ideal shape) which shows that this reconstruction method is efficient even in the presence of the phase-unwrapped errors of Fig 6(a)-(d).

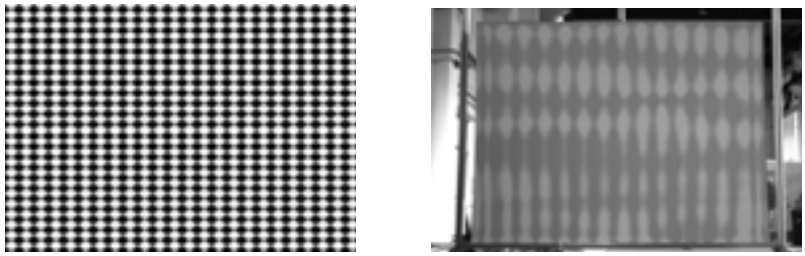

(a) (b)

Figure 5: (a) The two-dimensional pattern on screen; (b) The distorted pattern.

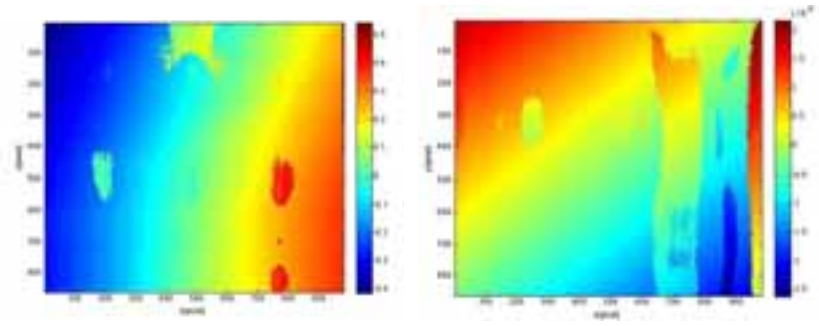

(a) (b)

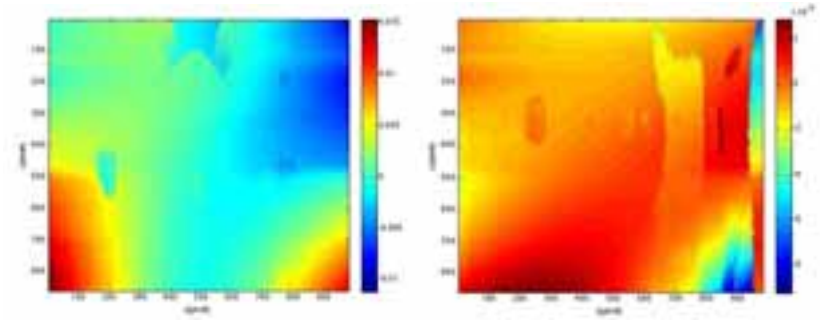

(c) (d)

Figure 6: (a) Slope distribution in the x-direction; (b) Slope distribution in the y-direction; (c) Slope error distribution in the x-direction; (d) Slope error distribution in the y-direction;

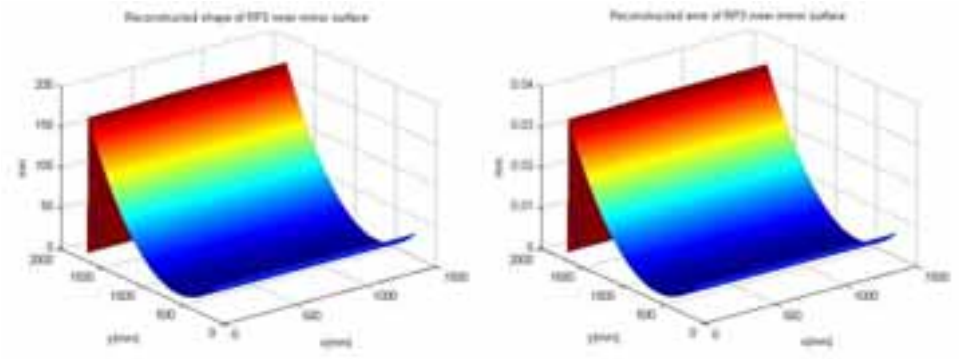

(a) (b)

Figure 7: (a) Reconstructed shape of RP3 inner mirror surface; (b) Reconstructed error.

7.Conclusion

In this paper, a solar collector surface measuring system based on orthogonal fringe reflection technique was built. The orthogonal fringe was projected onto a target screen and the deformed pattern modulated by the measured collector was captured by CCD camera. By establishing the mathematical relationship between phase difference and the gradient values of collector surface, the slope results were obtained. A shape reconstruction method based on approximation employing radial basis functions was proposed. Compared with the classical four-step phase shifting method, the proposed technique required only two fringe images to achieve 3D shape measurement of solar concentrator. The experiment measurement results demonstrated that not only were fine details preserved, but also the global shape was reconstructed as well, and even higher global accuracy. Furthermore, this measurement system made it possible to measure a large class of solar collectors.

Acknowledgements

The authors acknowledge the financial support from Supported by The National Natural Science Foundation of China (Grant No.61505211 and 51306171), The National Key Technology R&D Program (2012BAA05B02) .

References

1. Hansche B. Laser Ray Trace Tester for parabolic trough solar collectors. NDT Technology Division

9352, Sandia Laboratories, New Mexico, 1978, ISBN 87664-407-8.

2. Xiao J, Wei XD, Lu ZW, Yu WX, Wu HS. A review of available methods for surface shape measurement of solar concentrator in solar thermal power applications. Renewable and Sustainable Energy Reviews. 2012; 16:2539-2544.
3. Ulmer S, Marzr T, Prahl C, Reinalter W, Belhomme B. Automated High Resolution measurement of heliostat slope errors. Proceedings of the SolarPACES Conference. Berlin, Germany. 2009.
4. Marz T, Praul C, Ulmer S, Wilbert S, Weber C. Validation of two optical measurement methods for the qualification of the shape accuracy of mirror panels for concentrating solar systems. Journal of Solar Energy Engineering. 2011; 133:031022 1-7.
5. Ulmer S, Heinz B, Pottler K, Lupfert E. Slope error measurements of parabolic troughs using the reflected image of the absorber tube. Proceedings of the SolarPACES Conference. 2006.
6. Ulmer S, Marz T, Prahl C, Reinalter W, Belhomme B. Automated high resolution measurement of heliostat slope errors. Solar Energy. 2011; 85(4):681-7.
7. Zhu HB, Wang ZF, Wang HR. Novel method for shape measurement system of heliostat mirrors based on fringe reflection and its calibration. Proceedings of the SolarPACES Conference. Morocco. 2012.
8. Pottler K, Röger M, Lüpfert E, Schiel W. Automatic non-contact quality inspection system for industrial parabolic trough assembly. Journal of Solar Energy Engineering. 2008; 130(1):011008-5.
9. Pottler K, Lupfert E, Johnston G, Shortis MR. Photogrammetry: a powerful tool for geometric analysis of solar concentrators and their components. Journal of Solar Energy Engineering 2008; 127:94-101.
10. Roger M, Prahl C, Ulmer S. Fast determination of heliostat shape and orientation by edge detection and photogrammetry. Proceedings of the SolarPACES Conference. Las Vegas, NV USA, 2008.
11. Lehmann AG. Rapid heliostat surface measurement using reconstruction from camera images, Proceedings of the SolarPACES Conference. Granada, Spain, 2011.
12. Montecchi M, Benedetti A, Cara G. Fast 3D optical-profilometer for shape-accuracy control of parabolic-trough facets. Proceedings of the SolarPACES Conference. Granada, Spain, 2011.
13. Jones SA, Gruetzner JK, Houser RM, Edgar RM, Wendelin TJ. VSHOT Measurement Uncertainty and Experimental Sensitivity Study. Proceedings of the 32nd Annual Intersociety Energy Conversion Engineering Conference, Vol. 3, pp. 1877-1882.
14. Andraka C, Sadlon S, Myer B, Trapeznikov K, Liebner C. Rapid reflective facet characterization using fringe reflection techniques. Proceedings of the Energy Sustainability 2009, San Francisco, California, USA.
15. Diver RB, Moss T. Practical field alignment of parabolic trough solar concentrators. Journal of Solar Energy Engineering. 2009; 129:153-159.
16. Francini F, Fontani D, Sansoni P, Mercatelli L, Jafrancesco D, Sani E. Evaluation of Surface Slope Irregularity in Linear Parabolic Solar Collectors. International Journal of Photoenergy. 2012; pp 921780 1-6.
17. Wei T, Klette R. Height from gradient using surface curvature and area constraints. Third Indian Conference on Computer Vision, Graphics and Image Processing, 2002, pp. 204-210.
18. Wu Z, Li L. A line-integration based on method for depth recovery from surface normals. Computer Graphics and Image Process, 1988: 43, 53-66.
19. Ettl S, Kaminski J, Hausler G. Generalized hermite interpolation with radial basis functions considering only gradient data. Curve and Surface Fitting: Avignon 2006, Nashboro Press, 141-149.
20. Wendland H. Piecewise polynomial positive definite and compactly supported radial basis functions of minimal degree. Advances in Comp. Math, 1995: 4, 389-396.

21. Zhu H.B., Wang Z.F., Shape measurement and reconstruction of solar concentrator based on two-dimensional phase shift method, Energy Procedia, 69, 1921-1927, 2015.

22. Nitzan Goldberg, Amichai Zisken, Heliostat surface estimation by image processing, Proceedings of the SolarPACES Conference. Beijing, China, 2014.

23. S. Lowitzsch, J. Kaminski, M. C. Knauer, and G. Häusler, "Vision and modeling of specular surfaces," in Vision, Modeling, and Visualization 2005, G. Greiner, J. Hornegger, H. Niemann, and M. Stamminger, eds. (Akademische VerlagsgesellschaftAka GmbH, 2005), pp. 479–486.

24. Yang S.L., Chen Y.F., The Vector analysis and the application of fringe reflection method. National Cheng Kung University, Master thesis, 2007.